Modeling the Interference of Ultra-Wideband Signals in Multipath Propagation Channels

Jan-Philip Kniesel*, Sven Ole Schmidt† and Horst Hellbrück†
Luebeck University of Applied Sciences, Germany
Department of Electrical Engineering and Computer Science
* Email: jan-philip.kniesel@stud.th-luebeck.de
† Email: sven.ole.schmidt, horst.hellbrueck@th-luebeck.de

***Abstract*—Recently, one anchor Ultra-Wideband localization systems evolve as a new approach to determine the position of a tag with minimum infrastructure effort. The key of this method is to use a model of the propagation channel including the behaviour of multipath propagation. An issue of multipath propagation channels is, that signal echos can interfere at the receiver. To get a good model of the channel it is necessary to consider interference behaviour correctly. In this paper, we propose a model for Ultra-Wideband signals in multipath propagation channels that consider the phenomenon of interference and evaluate the model with measurements. We show that the proposed model is not able to represent a received signal in amplitude and signal shape completely correct. Additionally, we used the energy of a signal to compare the model and the measurement. We show that the changing of the energy due to different interference patters is represented by the model in a good agreement with the measurements.**

***Index Terms*—UWB, interference, multipath propagation**

I. Introduction and related work

In Internet of Things(IoT) systems, the localisation of movable devices is an important aspect, if the actual position is relevant to give measured information a context for their interpretation. Currently, several solutions exist for localisation systems [1]. One approach is to use the Ultra-Wideband technology (UWB), as the achievable accuracy is in the order of decimeter [2], due to large bandwidth and therefore a small symbol duration. On the other hand, infrastructure based localisation systems like in [2] yield to high deployment overhead [3]. Therefore, the goal of research is to hold the good accuracy of infrastructure based systems while reducing the deployment overhead. For UWB based localisation systems there exist approaches with low infrastructure effort like the single anchor system in [4]. The key of a single anchor system is to provide a good model of the channel impulse response(CIR). In [5] a model of a CIR is introduced. Due to multipath propagation in the channel, at the receiver it can come to the superposition of several signal echos and therefore to interference patterns. This must also be considered in the model for the CIR. The contributions of this paper are:

- We propose a model for the UWB impulse response that consider the phenomenon of interference
- We evaluate this model with measurements

The paper is organized as follows. Section II introduces multipath propagation and interference. In section III, a model for an UWB channel is proposed. Section IV provides the evaluation of the model with measurements. Section V concludes the paper and gives an outlook for future work.

II. Theory

This section introduces multipath propagation and interference

A. Multipath propagation

In multipath propagation systems a transmitted signal $x(t)$, in form of an electromagnetic wave, reaches the receiver not only on the direct but also on several indirect paths. This circumstance is shown in Figure 1. On the one hand, the signal from the TX-antenna reaches the RX-antenna directly on the shortest possible path, this is called the line of sight (LOS) path. On the other hand, the signal could reach the RX-antenna over the ground reflection and a reflection at a wall. These paths are called the none line of sight (NLOS) paths. The total received signal $y(t)$ is the additive superposition of the LOS and all NLOS echos. This additive superposition of electromagnetic waves leads to interference patterns.

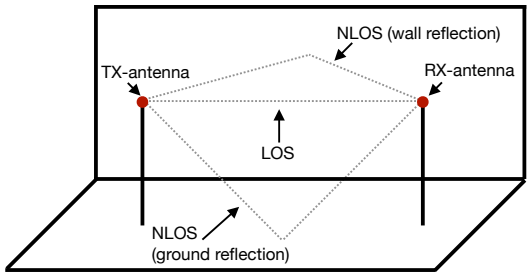

Fig. 1: Sketch of multipath propagation, including one LOS path and two NLOS paths

B. Interference of signals

Interference is the phenomenon, that two or more signals superpose and the resulting signal has a larger or smaller amplitude than the original signals. This effect is shown in Figure 2. The plot shows two different signals (blue and red) and their resulting superposition (yellow). The yellow signal is calculated from the addition of the two other signals. For

example, in the interval from 2.5 ns to 3 ns, the yellow signal has a smaller amplitude than the original parts. This is called destructive interference. Otherwise, if the resulting signal has a larger amplitude, the phenomenon is called constructive interference. The energy of a signal $h(t)$ inside the interval from t_0 to t_1 is given by $E = \int_{t_0}^{t_1} h(t)^2 dt$. Due to the lower amplitudes, destructive interference decreases the energy, and constructive interference increases the energy of a signal.

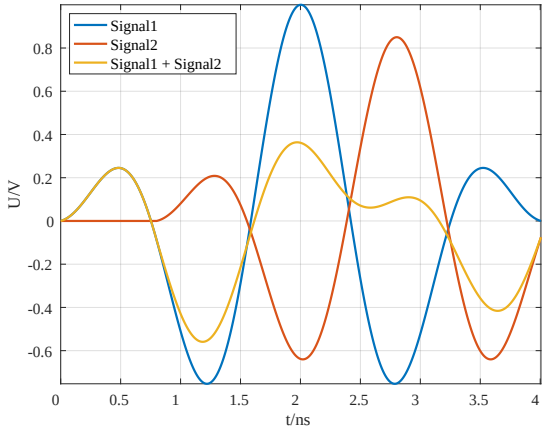

Fig. 2: Plot of two signals and there additive superposition

III. Model of Multipath Propagation and Interference

In this section, a model is proposed, that handles the multipath propagation and the interference in UWB transmission channels.

First, the UWB transmitting signal is modelled. We use for this paper the standardised UWB Channel 2 [6], where the impulse has a bandwidth of $f_b = 499.2\,\mathrm{MHz}$ and a center frequency of $f_c = 3.9936\,\mathrm{GHz}$. The amplitude has in this case a value of $\hat{x} = 300\,\mathrm{mV}$. The modelled UWB impulse x(t) is then described by the following equation:

$$x(t) = \begin{cases} \hat{x} \cdot \mathrm{sinc}(t \cdot f_b - 1)\cos(2\pi f_c t) & \text{if } 0 \leqslant t \leqslant \frac{2}{f_b} \\ 0 & \text{else} \end{cases} \quad (1)$$

The sinc-function is the baseband signal and has a spectrum that equals a rectangular with a width of f_b. The cos-function shifts the baseband signal in the spectrum to the desired centre frequency f_c. The signal $x(t)$ is depicted in Figure 3. The orange curve shows the UWB impulse in the baseband and the blue curve the UWB impulse shifted to the center frequency.

The next step is to model the channel impulse response(CIR) $h(t)$. The CIR is the response of the channel when a Dirac delta impulse $\delta(t)$ is transmitted. A simple approach to model $h(t)$ is described in [5]:

$$h(t) = \sum_{n=1}^{3} a_n \cdot \delta(t - \tau_n)(-1)^{k_n} \quad (2)$$

As seen in eq.(2), in general $h(t)$ is the superposition of time shifted and weighted Dirac delta impulses. The different time

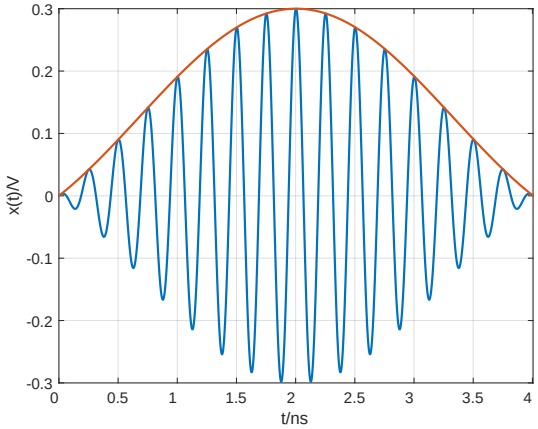

Fig. 3: Plot of the UWB impulse $x(t)$, given by eq.(1)

shifts τ_n results from the different length d_n of the LOS and NLOS paths and are calculated with $\tau_n = \frac{d_n}{c}$. The single components of $h(t)$ are attenuated depending on the length of the path. Assuming the free space model, the attenuation factors a_n are calculated with:

$$a_n = \sqrt{\left(\frac{\lambda}{4\pi d_n}\right)^{\gamma}} = \sqrt{\left(\frac{1}{4\pi \tau_n f_c}\right)^{\gamma}} \quad (3)$$

The coefficient γ is an environment depending parameter and is set to 2.278, as the environment in that Schramm et. al. [7] determined the coefficient is very similar to our measurement environment. Every reflection of a signal causes a phase shift of 180°, this is equal to an alternating sign. In eq.(2) the phase shifts due to reflections are modelled with the term $(-1)^{k_n}$ $k_n \in \mathbb{N}_0$, where k_n is the number of reflections of the single signal components. As we consider the LOS path and two NLOS paths (ground and one wall reflection), the maximum value of n is three. This is a simplification of the real CIR.

The channel response $y(t)$ of the UWB impulse is the convolution of the UWB impulse $x(t)$ from eq.(1) and the CIR $h(t)$ from eq.(2):

$$y(t) = (x * h)(t) \quad (4)$$

In Figure 4 the received signal $y(t)$ is shown for two exemplary CIR $h_1(t)$ and $h_2(t)$. $h_1(t)$ is selected to show the case where the two NLOS echos do not overlap. In contrast, $h_2(t)$ is selected to show the case where the two NLOS echos overlap and therefore interfere. The interference behaviour in this case is constructive.

In the next section, this model is evaluated by comparison with a real measurement.

IV. Evaluation

In this section, the measuring setup is described and the measurement output is compared with the corresponding model output.

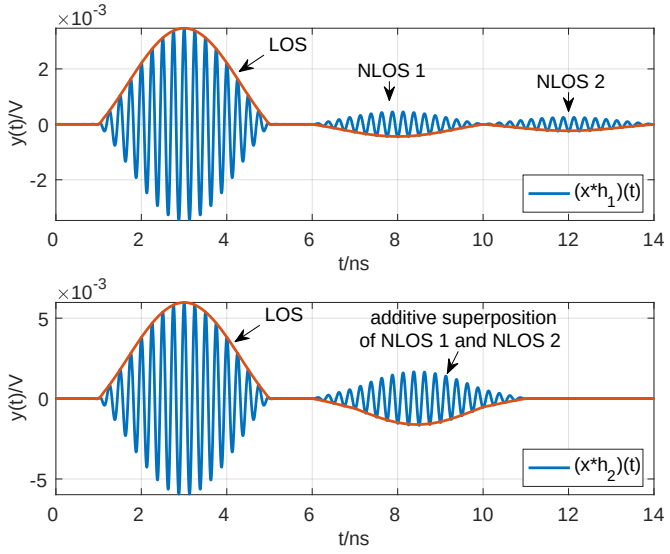

Fig. 4: Plot of two different signals $y(t)$, calculated with eq.(4)

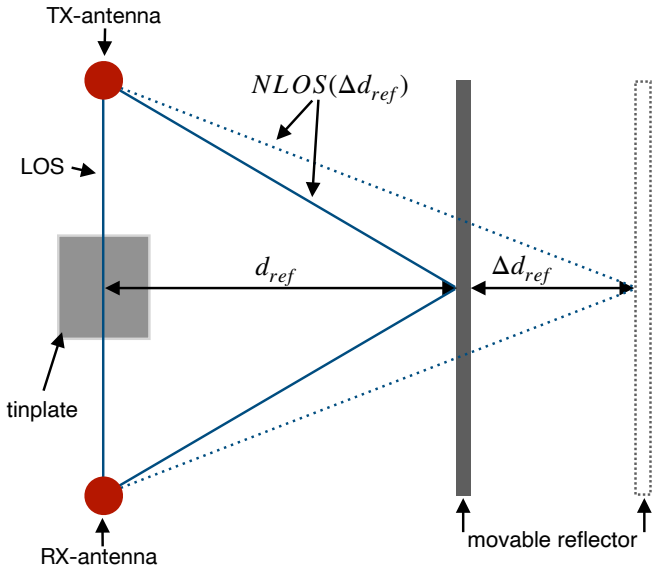

Fig. 5: The top view of the measuring setup

A. *Measurement setup*

The top view of the measuring setup is shown in Figure 5. Two antennas (Decawave WB002[8]) are placed at a distance of $d_{LOS} = 0.45\,\mathrm{m}$ from each other and at a height of $h = 1.1\,\mathrm{m}$. A movable reflector is installed at a distance of $d_{ref} = 0.95\,\mathrm{m}$. On the ground, between the two antennas, a piece of tinplate ($0.45\,\mathrm{m}$ thick) is placed to reduce the effect of reflection losses. With this setup, the CIR has one LOS path and two NLOS paths (over the tinplate on the ground and over the reflector). Although the measurements were carried out in a furnished laboratory environment we assume that other signal echos have a negligible influence on the CIR. This is reasonable, since we ensured that the distance of the NLOS paths caused by other obstacles in the room were much larger than the intended NLOS paths.

A signal generator (Tektronik AWG 70000A[9]) generates the UWB impulse $x(t)$ from eq.(1), over the TX-antenna the signal is transmitted. The signal $y(t)$, received by the RX-antenna, is analysed with an oscilloscope (Tektronik DPO 70000[10]). The values for d_{ref}, h and d_{LOS} are determined so that the two NLOS paths have approximately the same length and therefore the echos interfere at the receiver. Moving the reflector yields to different interference patterns, because the length of the NLOS path over the reflector changes depending on Δd_{ref}. We did the measurements with a reflector moving in $1\,\mathrm{mm}$ steps over a distance of $30\,\mathrm{cm}$. For each reflector position, the UWB impulse was sent and measured 1000 times and the arithmetic mean out of these measurements was calculated.

B. *Comparison between the model and the measurement data*

Additionally to the measurements with the reflector, one measurement without the reflector was made. This idle measurement is applied to show the differences between the model and the measurements without the interference effects due to the reflector NLOS part. In Figure 6, the idle measurement results are shown.

As can be seen, there are differences between the modelled and

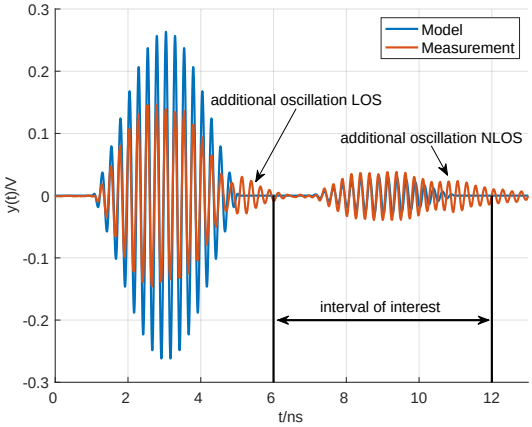

Fig. 6: Measured and modelled idle signal

the measured signal. The amplitude of the LOS signal of the model does not really fit to the LOS signal of the measurement. This difference of the amplitudes is also present analysing the NLOS echos, but not that strong. This indicates, that the attenuation parameters of the model do not represent the real attenuation correctly. Furthermore, in the measurements it can be seen, that there is an additional oscillation after the original impulses, that is not considered in the model. This effect, most probably, comes from the non-perfect receiving or transmitting antenna and is to be investigated in further research. Ignoring the additional oscillation, the pulse widths of the model and the measurement are in good agreement and it is also positive, that the signals are almost in phase and have approximately the same frequency.

To investigate the interference behaviour of the NLOS echos it is not necessary to look at the whole receiving signal but only at the part where the interference really takes place. Therefore, in Figure 6 the interval of interest is drawn in, where the following investigations refer to.
In section II it is explained, that due to the effect of interference it comes to varying amplitudes yielding to change of the energy of the signal. This must also be seen in the model if it represents the interference effect right. As already mentioned, the model is not really optimised regarding the amplitude and the additional oscillation. Therefore, also the absolute energy of the model differs from the energy of the measurements. To compare the changes of the energy of the signals due to the different interference patterns, it is reasonable to normalize the values. In this case, the values are normalized to the maximum energy value of the model respectively the measurements. The energy of the receiving signal inside the interval of interested depending on the position of the reflector is shown in Figure 7. As expected, the energy changes depending on the actual

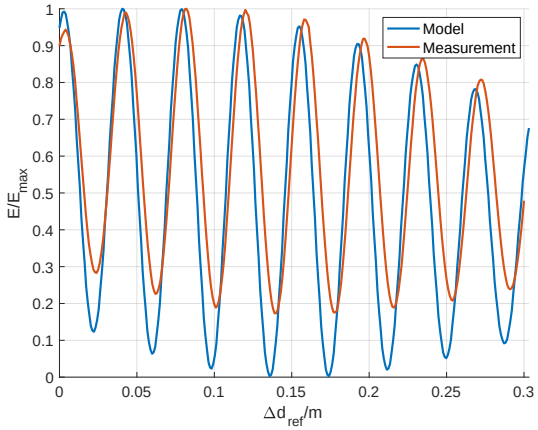

Fig. 7: Investigation of the energy of the modelled and measured signal inside the interval of interest

reflector position and therefore the actual interference pattern. There are positions where the energy has a minimum, caused by the destructive interference of the NLOS paths. And there are positions where the energy has a maximum, caused by a constructive interference of the two NLOS paths. This behaviour can also be seen with the modelled signal and moreover the period of the modelled energy oscillation is similar to the period of the measured signal. Looking at the peak to peak values there is still a difference between the model and the measurement.

V. Conclusion and Future Work

The results from Figure 7 indicates, that the affect of interference is basically represented by the model, but that there are more parameters that are not taken into account by the model. These unknown parameters effect the differences to the real measurements.

The model that is proposed in this paper can not describe the corresponding measurements completely correct. The main issues of the model are the wrong amplitude and the additional oscillations. Besides that, it is shown, that the approach to model the UWB-impulse response with eq.(4) considered basically the phenomenon of interference. In future work, the two issues must be solved, to become a more realistic model that is suitable for one anchor localisation systems.

Acknowledgments

This publication is a result of the research of the Center of Excellence CoSA and funded by the Federal Ministry for Economic Affairs and Energy of the Federal Republic of Germany (BMWi FKZ ZF4186108BZ8, MOIN). Horst Hellbrück is adjunct professor at the Institute of Telematics of University of Lübeck.

References

[1] H. Liu, H. Darabi, P. Banerjee, and J. Liu, "Survey of wireless indoor positioning techniques and systems," *IEEE Transactions on Systems, Man, and Cybernetics, Part C (Applications and Reviews)*, vol. 37, no. 6, pp. 1067–1080, 2007.

[2] B. Kemke, P. Pannuto, and P. Dutta, "Polypoint:guiding indoor quadrotors with ultra-wideband localization," *Proc. of the 2nd Int. Workshop on Hot Topicsin Wireless (HotWireless)*, 2015.

[3] D. Lymberopoulos and J. Liu, "The microsoft indoor localization competition: Experiences and lessons learned," *IEEE Signal Processing Magazine*, vol. 34, no. 5, pp. 125–140, 2017.

[4] B. Großwindhager, M. Rath, J. Kulmer, M. S. Bakr, C. A. Boano, K. Witrisal, and K. Römer, "Salma: Uwb-based single-anchor localization system using multipath assistance," in *Proceedings of the 16th ACM Conference on Embedded Networked Sensor Systems*, ser. SenSys '18. New York, NY, USA: Association for Computing Machinery, 2018, p. 132–144. [Online]. Available: https://doi.org/10.1145/3274783.3274844

[5] 4th KuVS/GI Expert Talk on Localization, Lübeck, Germany, 11.-12. Juli 2019, B. Matthews, S. O. Schmidt, and H. Hellbrück, "Understanding and prediction of ultra-wide band channel impulse response measurements," *Proceedings of the 4th KuVS/GI Expert Talk on Localization*, 2019. [Online]. Available: https://publikationsserver.tu-braunschweig.de/receive/dbbs_mods_00066765

[6] "Ieee standard for low-rate wireless networks," *IEEE Std 802.15.4-2015 (Revision of IEEE Std 802.15.4-2011)*, pp. 1–709, 2016.

[7] S. Schramm and S.Schmidt, "Modeling the path losses of ultra-wideband signals in multipath propagation channels," 2021.

[8] Decawave, "Decawave antenna design," Feb. 2021. [Online]. Available: https://www.decawave.com/uwb-antennae-design-files/

[9] Tektronix, "Awg70000a series datasheet," Feb. 2021. [Online]. Available: https://download.tek.com/datasheet/AWG70000A-Arbitrary-Waveform-Generator-Datasheet-76W283808.pdf

[10] ——, "Mso/dpo70000 series datasheet," Feb. 2021. [Online]. Available: https://www.tek.com/datasheet/digital-and-mixed-signal-oscilloscopes